Isı Bilimi ve Tekniği Dergisi, 38, 1, 11-24, 2018
J. of Thermal Science and Technology

ISSN 1300-3615

A COMPARATIVE ASSESSMENT OF TURBULENT FORCED CONVECTION HEAT TRANSFER FROM A SINGLE CYLINDER USING RANS AND LES MODELS

Zekeriya ALTAÇ and Necati MAHİR
Eskişehir Osmangazi University, School of Engineering and Architecture,
Mechanical Engineering Department, Batı-Meşelik, 26480, Eskişehir.
zaltac@ogu.edu.tr, nmahir@ogu.edu.tr

(Geliş Tarihi: 14.03.2017, Kabul Tarihi: 23.10.2017)

Abstract: Unsteady 2D and 3D turbulent flow and heat transfer characteristics of a single isothermal horizontal cylinder in crossflow of air (Pr=0.7) is investigated to assess the numerical performance of the common turbulence models currently in use. For 2D simulations, Standard k–ε (SKE), Re-Normalization Group k–ε (RNG), Realizable k–ε (RKE), Standard k-ω (SKW), Shear Stress Transport (SST) k-ω and Reynolds Stress Model (RSM) turbulence models are used in conjunction with the two-layer wall (or Enhanced Wall Treatment, EWT) model. For 3D simulations, RNG, SKW, SST, RSM and Large Eddy Simulation (LES) using Smagorinsky-Lilly with and without dynamic stress models are used. In this study, the performance criterion of the turbulence models is based on the accuracy of the computational predictions of 2D and 3D flow as well as heat transfer (C_D, C_L, $C_{L,rms}$, St and Nu numbers) characteristics. Numerical simulations are carried out for Reynolds numbers of 1000, 3900 and 10000 using FLUENT 6.3.26® CFD software. The flow characteristics, such as the lift/drag coefficients and Strouhal numbers, are computed and tabulated comparatively with available experimental and numerical data. The 2D RANS models are not consistent in predicting the flow characteristics due to three-dimensionality nature of the fluid flow, but RSM performs slightly better than RANS models. The mean Nusselt number for Re=1000 and 3900 is predicted with reasonable accuracy with 2D-RANS models. While the RNG model consistently over estimates the mean Nusselt number, other 3D-RANS models yield values within the ranges predicted by the Nusselt number correlations. It is shown that although LES models yields reasonable flow and heat transfer characteristics for flow conditions considered here, the performance of LES is also dependent on the inlet condition.
Keywords: Large eddy simulation, turbulence models, two-dimensional, three-dimensional, RANS models.

BİR SİLİNDİRDEN ZORLANMIŞ TÜRBÜLANSLI TAŞINIM ISI GEÇİŞİNDE RANS VE LES MODELLERİNİN KIYASLAMALI BİR DEĞERLENDİRMESİ

Özet: Geçici rejimde çapraz hava (Pr=0.7) akışına maruz izotermal yatay bir silindirin 2B ve 3B türbülanslı akış ve ısı geçiş karakteristikleri halihazırda yaygın olarak kullanılan türbülans modellerinin sayısal performansı bağlamında araştırılmıştır. 2B simülasyonlar için Standard k–ε (SKE), Re-Normalizasyon Grup k–ε (RNG), Realizable k–ε (RKE), Standard k-ω (SKW), Shear Stress Transport (SST) k-ω and Reynolds Stress Modeli (RSM) türbülans modelleri iki-tabaka duvar (veya Gelişmiş Duvar Uygulaması) modeli ile birlikte kullanılmıştır. 3B simülasyonlar için, RNG, SKW, SST, RSM ve dinamik gerilme modeli içeren ve içermeyen Smagorinsky-Lilly algoritması kullanan LES modeli kullanılmıştır. Bu çalışmada, türbülans modeleri için performans kriteri 2B ve 3B akış ile ısı geçişi sayısal tahminlerin doğruluğuna (C_D, C_L, $C_{L,rms}$, St ve Nu sayıları) dayanmaktadır. FLUENT 6.3.26® CFD yazılımının kullanıldığı sayısal simülasyonlar, Reynolds sayılarının 1000, 3900 ve 10000 değerleri için gerçekleştirilmiştir. Kaldırma/sürünme katsayıları ve Strouhal sayıları gibi akış karakteristikleri hesaplanarak mevcut deneysel ve sayısal verilerle karşılaştırmalı olarak kıyaslanmıştır. 2B RANS modelleri, akışın doğası gereği üç boyutlu olması nedeniyle akış karakteristiklerinin tahmininde tutarlı değildir, ancak RANS modellerine nazaran RSM biraz daha iyi bir performans göstermiştir. 2B RANS modellerinde Re=1000 ve 3900 için ortalama Nusselt sayısı makul bir doğrulukla tahmin edilmiştir. RNG modeli tutarlı bir şekilde ortalama Nusselt sayısını yüksek tahmin etmekte iken, diğer 3B-RANS modelleri mevcut Nusselt korrelasyonlarının tahmin aralığında sayısal sonuçlar vermiştir. LES modelinin, bu çalışmada göz önüne alınan akış koşullarında, makul akış ve ısı geçişi karakteristikleri ile sonuçlanmasına rağmen LES'in performansı giriş koşullarına da bağlı olduğu gösterilmiştir.
Anahtar Kelimeler: LES simulasyonu, türbülans modelleri, iki-boyutlu, üç-boyutlu, RANS model.

NOMENCLATURE

A	area (m^2)
C_D, C_L	drag and lift coefficients
D	side length of the cylinder [m]
F_D, F_L	drag and lift force [N]
h	heat transfer coefficient [W/m^2K]
I	turbulence intensity
k	thermal conductivity [W/mK]
Nu	Nusselt number [$=hD/k$]
P	Pressure [Pa]
Pr	Prandtl number [$=\upsilon/\alpha$]
Re	Reynolds number [$=U_\infty D/\upsilon$]
t	time [s],
T	temperature [K]
u_j	velocity components [m/s]
U_∞	free stream velocity [m/s]
x_j	dimensionless coordinates,

Greek symbols

α	thermal diffusivity [m^2/s]
β	viscosity ratio μ_t/μ
μ	viscosity (Pa. s)
υ	kinematic viscosity [m/s^2]
ρ	density [kg/m^3]
τ	dimensionless time

Subscripts

rms	root mean square
t	turbulence
w	wall
∞	free stream

INTRODUCTION

The flow past a circular cylinder in a uniform free stream is regarded as the standard bluff body flow. In many engineering practices, a cylinder is used as a heat transfer surface where the mainstream flow around the cylinder contains a high level of velocity fluctuations. Despite the simplicity of the geometry, the flow is complicated which exhibits large diversity in its behavior in the form of a strong dependence on the Reynolds number, as well as a strong sensitivity to small perturbations in the flow. For these reasons, the flow over a circular cylinder has been the subject of many experimental and numerical studies over the last 60 years in most part for two reasons: (i) the geometry is simple and (ii) many complex and interesting flow phenomena occur in the wake of the cylinder.

Despite the large number of investigations, our understanding of flow past circular cylinder flow is still incomplete. Due to its commonality in many engineering fields, there is abundant data in the literature for comparisons when validating numerical techniques in the laminar flow range. Three-dimensionality of the flow, however, becomes important above Re≈200; therefore, more recent studies at high Reynolds numbers have made use of 3D computational models. Recent increase in computation capabilities has also prompted numerical studies involving turbulent flow passed circular cylinders.

Earliest experimental studies on the flow characteristics of a cylinder in cross flow date back the begining of 20th century. Niemann and Hölscher (1990) provided a comprehensive review of the experimental studies on this topic up until 1990. The most recent review was carried out by Williamson and Govardhan (2004). Gerrard (1961) experimentally studied the oscillating lift and drag forces on circular cylinders in the range of Reynolds number from 4000 to 10^5. Rhosko (1961) performed measurements on a large circular cylinder in a wind tunnel at Reynolds numbers from 10^6 to 10^7 to determine the drag coefficient. Achenbach (1968) experimentally studied the flow around single cylinders in the range of Reynolds numbers $6\times10^4 < Re < 5\times10^6$. Kacker et al. (1974) measured the fluctuating lift and drag forces for cylinders in cross flow in the range $Re=10^4$ to 2.5×10^5. For Reynolds numbers ranging from 2×10^4 to 3×10^5, Norberg and Sunden (1987) investigated experimentally the flow around a circular cylinder. Norberg (1994) experimentally investigated the Strouhal number and the mean base suction coefficient for the Reynolds numbers from about 50 to 4×10^4 where different aspect ratios. Dong et al. (2006) investigated flow around a cylinder experimentally imaging (PIV) and direct numerical simulations at Re= 3900/4000 and 10000. Norberg (2003) provided additional experimental data on the lift coefficients and St numbers with fitted correlations for a circular cylinder in cross flow in addition to reviewing previously published ones, for the Re=47 to 2×10^5.

Two-dimensional numerical simulation of a cylinder in cross turbulent flow is limited in the literature. Among rare 2D studies, Çelik and Shaffer (1995) used standard k-ε (SKE) model for the prediction of time average flow over circular cylinder for Reynolds numbers between 10^4–10^7. Henderson and Karniadakis (1995) used a spectral element-Fourier algorithm for simulating Re=1000 flows in complex geometries using unstructured grids. Selvam (1997) used an implicit procedure for solving 2D Large Eddy Simulation (LES) to compute the drag and Strouhal numbers for $Re=10^4$, 10^5, 5×10^5 and 10^6. Rahman et al. (2007) numerically investigated the characteristics of unsteady 2D laminar and turbulent wakes behind a circular cylinder for Re=1000 and 3900. Standard *k*-ε, Realizable *k*-ε (RKE) and Shear-Stress Transport (SST) *k*-ω turbulence models were used to assess the capabilities of these turbulence models in the computation of the lift and drag coefficients. Ong et al. (2009) investigated high Re number flow (10^6, 2×10^6, 3.6×10^6) around a circular cylinder using 2D-Unsteady Reynolds Averaged Navier-Stokes (URANS) SKE model. Ünal et al. (2010) comparatively studied the effect of Spalart Allmaras (SA), SKW, RKE and SSTKW models in predicting flow field near wake of circular cylinder at Re=41300. Saghafian et al. (2003) employed a nonlinear eddy-

viscosity model to 2D flow over circular cylinders for $10^3 \leq Re \leq 10^7$.
The use of RANS models in a 3D turbulent flow analysis of a circular cylinder in cross flow is also rare. For Re=3900, Young and Ooi (2007) showed that using a 3D URANS model results in minor improvement over 2D model for flow over a cylinder, and using a LES model results in significant gain in bulk quantities. Benim et al. (2008) numerically investigated the predictability of the drag coefficient in turbulent flow past a circular cylinder using 2D and 3D RANS, 2D and 3D URANS, LES and Detached Eddy Simulation (DES).

Majority of 3D CFD analysis of a circular cylinder in cross flow involves LES models. Kalro and Tezduyar (1997) presented 3D finite element computation of unsteady flows around circular cylinders. For $Re=10^4$, they employed LES turbulence model. For Re=3900, the turbulent flow over a circular cylinder was computed by Breuer (1998) using 2D and 3D LES. Fröhlich et al. (1998) presented LES computations of Re=3900 and 140000 using structured FVM and unstructured FEM methods to assess the performance and the potential of the two methods. Kravchenkoa and Moin (2000) studied the flow over a circular cylinder at Reynolds number 3900 using the LES. Franke and Frank (2002) employed LES for the turbulent flow around a circular cylinder at Re=3900. Shim et al. (2009) numerically studied the flow past a circular cylinder at Re=3900 using 3D LES as well as URANS models. Patel (2010) investigated flow past single cylinders for Re=1000 and 3900. Ouvrard et al. (2010) studied the effects of numerical viscosity, subgrid scale (SGS) viscosity and grid resolution in LES and VMS-LES for the flow around a circular cylinder at Re=3900. Mustto and Bodstein (2011) studied 2D turbulent flow passed a circular cylinder in the Reynolds number range from 10^4 to 6×10^5. Kim et al. (2012) studied the effect of the discretization in turbulent flow around a circular cylinder is assessed at Re=10000 in using 3D LES. Variational multiscale large-eddy simulations (VMS–LES) of the flow around a circular cylinder were carried out at by Wornom et al. (2011) for Re = 3900, 10^4 and 2×10^4. The Wall-Adapting Local Eddy-viscosity (WALE) subgrid scale model was used to account for the effects of the unresolved scales. Sidebottom et al. (2015) studied the flow past a circular cylinder for Re=3900 using LES to assess the affect of subgrid scale (SGS) turbulence models, wall models, discretization of the advective terms. Kim et al. (2015) carried out 3D unsteady large-eddy simulation using two different subgrid scale models for Re=5500–41300. Lysenko et al. (2012) solved the flow over a circular cylinder for Re=3900 by using LES. Parnaudeau et al. (2008) investigated the flow over a circular cylinder at Re=3900 both numerically with LES and experimentally with hot-wire anemometry and particle image velocimetry.

Experimental and numerical investigations involving forced convection heat transfer from a single cylinder in cross flow have similarly attracted attention for the last several decades. Morgan (1975) has summarized the experimental heat transfer work on smooth circular cylinders up until 1975. Boulos and Pei (1973) also reviewed the experimental and theoretical work on the transfer of heat and mass between a circular cylinder and a turbulent fluid stream in cross flow for the Reynolds number range from 10^3 to 10^5. Ahmed and Yonanovich (1997) experimentally studied the forced convection heat transfer from different body shapes with respect to the Reynolds number and different characteristic body lengths, and empirical models for forced convection heat transfer were presented. Scholten and Murray (1998a) experimentally studied the time resolved heat flux and local velocity at the surface of a cylinder in cross flow for $7000<Re<50000$. In a follow up paper (1998b), tests with high freestream turbulence, it was reported that transition to turbulence occurred within the boundary layer of the cylinder for a range of Reynolds numbers. Unsteady heat transfer from a circular cylinder to the cross-flow of air was investigated by Nakamura and Igarashi (2004) experimentally for Reynolds numbers from 3000 to 15,000. They showed that the heat transfer in the separated flow region has spanwise nonuniformity throughout the examined Reynolds number range. Pasinato (2008) numerically investigated the flow with heat transfer around a circular cylinder at for Re=3900 and Pr=0.71 using LES (Smagorinsky-Lylli model). They found that mean Nusselt number error was in the order of 20% with experimental data, and the local heat transfer prediction exhibited a poor performance in the separated region. Bose et al. (2012) studied the accuracy of eddy diffusivity subgrid scale model for large-eddy simulation of passive scalar transport is investigated for a heated cylinder in crossflow at Re=3000 and 8900.

With the availability and increased usage of commerical softwares in R&D, 2D/3D turbulence models are at the disposal of non-expert end users as well. In the absence of informative literature on the conditions and usage of turbulence models, the numerical analyst is faced with the dilemma of choosing reliable and appropriate turbulence models at hand. Engineering design considerations are primarly concerned with obtaining the flow characteristics such as drag/lift coefficient and Strouhal number, and the mean Nusselt number as the heat transfer characteristic. The main objectives of this study can be viewed in two folds. First is to assess the accuracy of turbulence flow simulations using 2D SKE, RKE, RNG, SKW, SST and RSM models and to determine the models that predict the heat transfer (i.e., Nusselt number) closest with respect to those of the experimental and 3D numerical simulations. Besides filling voids in the literature in this respect, the flow characteristics (C_D, C_L, St number) are also computed with each turbulence model to validate and compare with readily available data. Second is to assess the numerical performance of the 3D RANS (RNG, SKW, SST and RSM), as well as LES (Smagorinsky-Lilly

with/withouth dynamic stress) models, in terms of the performance of the heat transfer predictions.

NUMERICAL SIMULATIONS

Governing Equations

The unsteady flow and heat transfer analysis is numerically simulated using commercial software FLUENT® 6.3.26 (Fluent, 2006). The turbulence models featured in FLUENT® are covered in the literature, as well as in pertinent Users' Guide. For this reason, the governing equations, and the major features of the LES and RANS models will be briefly mentioned here to save space.

The fluid flow is described by the RANS equations and the time averaged-energy equation for the mean temperature field—using tensor notation—are reduced to the following forms:

$$\frac{\partial u_j}{\partial x_j} = 0 \tag{1}$$

$$\frac{Du_i}{Dt} = -\frac{1}{\rho}\frac{\partial P}{\partial x_i} + \frac{\partial}{\partial x_j}\left(\upsilon\frac{\partial u_j}{\partial x_j} - \overline{u_i' u_j'}\right) \tag{2}$$

$$\frac{DT}{Dt} = \frac{\partial}{\partial x_j}\left(\alpha\frac{\partial T}{\partial x_j} - \overline{T' u_j}\right) \tag{3}$$

where D/Dt is the material derivative, T is the temperature, P is the pressure, ρ is the fluid density, α is the thermal diffusivity, υ is the kinematic viscosity, and $\overline{u_i' u_j'}$ and $\overline{T' u_j}$ are the turbulent stress and heat flux which are modeled by the turbulence models.

The lift and drag coefficients and forces on a cylinder are computed from

$$C_{\mathrm{L}} = \frac{F_D}{\frac{1}{2}\rho U_\infty^2 A}, \qquad C_{\mathrm{D}} = \frac{F_L}{\frac{1}{2}\rho U_\infty^2 A} \tag{4}$$

where F_D and F_L are the drag and lift forces and A is the projected area. The Reynolds number is defined as $\mathrm{Re} = U_\infty D/\nu$ while the local heat transfer coefficient and the local Nusselt number are computed from

$$-k\left(\frac{\partial T}{\partial n}\right)_w = h_{\theta,z}\left(T_w - T_\infty\right), \qquad \mathrm{Nu}_{\theta,z} = \frac{h_{\theta,z} D}{k} \tag{5}$$

where A is the cylinder side surface area.

Turbulence Models

In this study, the following are considered in the assessments of performance of turbulence models.

Standard k−ε Model (SKE): This model, proposed by Launder and Spalding (1972), is a simple complete turbulence model where the solution of two separate transport equations allows the turbulent kinetic energy and length scales to be independently determined. The theory of the SKE model is well established in the literature, and it is widely used in practical industrial flows and heat transfer calculations due to its robustness, economy and reasonable accuracy. This model assumes fully turbulent flow and neglects the effects of molecular viscosity. The model requires an additional model for the near-wall where wall-functions based on semi-empirical formulas and functions are employed. The strengths and weaknesses of the SKE model are well known.

RNG k−ε Model (RNGKE): The RNG k−ε model (Yakhot and Orszag, 1986) is developed from the renormalization group theory. It includes several refinements over the SKE model. That is, the effect of swirl on turbulence is included in the RNG model, and an additional term supplied in the ε-equation significantly improves the accuracy for rapidly strained flows. The RNG theory also provides an analytical expression for the turbulent Prandtl numbers. These features have been observed to yield more accurate and reliable solutions for a wider class of flows than the SKE model.

Realizable k−ε Model (RKE): It is a variant of SKE model (Shih et. al., 1995). The term "realizable" means that the model satisfies certain mathematical constraints (consistent with the physics of turbulent flows) imposed on the Reynolds stresses. This model contains a formulation for the turbulent viscosity, and for the dissipation rate, a new transport equation is derived from an exact equation for the transport of the mean-square vorticity fluctuation. Both the RKE and RNGKE models exhibit improvements over SKE model. Due to its relatively recent introduction to CFD calculations, it is not clear in which cases the RKE model outperforms the RNGKE model.

Standard k−ω Model (SKW): This model is based on the Wilcox *k*-ω model (Wilcox, 1998) which incorporates modifications for low-Re number effects, compressibility and shear flow spreading. It is one of the most common models, and the turbulent kinetic energy equation is similar to that of the SKE model. ω which is the specific dissipation determines the scale of turbulence. The model predicts free shear flow spreading rates that are in close agreement with measurements for far wakes, mixing layers, and plane, round and radial jets. It is thus applicable to wall-bounded flows and free shear flows.

Shear-Stress Transport k−ω Model (SSTKW): This model was developed by Menter (1994) to effectively blend the robust and accurate formulation of the SKW model in the near-wall region with the free-stream independence of the SKW model in the far field. To achieve this, the k−ε model is converted into a k−ω formulation. The definition of the turbulent viscosity is modified to account for the transport of turbulent shear stress.

Reynolds Stress Model (RSM): The Reynolds stress model is the most elaborate turbulence model. The

Reynolds stresses are directly computed (Fluent, 2006). The exact Reynolds stress transport equation accounts for the directional effects of the Reynolds stress fields. The method has the potential to produce more accurate predictions for complex flows; however, the computational costs far exceed other RANS models. The method has not been widely validated as much as the k−ε models due to its computational burden. The major uncertainty comes from the modeling of the turbulent dissipation, and it may not always yield better results in comparison to the simpler models.

Large-Eddy Simulation (LES): LES which does not adopt the conventional time- or ensemble-averaging RANS approach with additional modeled transport equations was proposed by Smagorinsky. In LES, the large scale motions of turbulent flow are computed directly and only small scale (sub-grid scale SGS) motions are modeled (Fluent, 2006). Since most of the turbulent energy is contained in large eddies, LES is more accurate than the RANS approaches and captures these eddies in full detail. Furthermore, the small scales tend to be more isotropic and homogeneous than the large ones, and thus modeling the SGS motions is easier than modeling all scales within a single model as in the RANS approach. Currently LES seems to be the most viable/promising numerical tool for simulating realistic turbulent/transitional flows.

Wall functions

In the region near the wall, the velocity and temperature gradients are steep, and numerical modeling requires fine grids near the wall in order to accurately simulate the changes in temperature and velocity components. For the RANS models, the two-layer model which is incorporated into FLUENT as Enhanced Wall Treatment (EWT) is used for near-wall modeling; the near-wall region is divided into two—viscous and fully turbulent—sublayers based on the turbulent Reynolds number. This wall-model allows to resolve the viscous sub layer with very fine mesh (at first near-wall node $y^+\approx 1$ where y^+ is dimensionless distance from the wall defined as yu/v). The two-layer approach is used to specify both ε and the turbulent viscosity in the near-wall cells. The same grid configurations were used in numerical simulations of models used in the study.

Modeling and Computational Aspects

The 2D computational domain considered, $30D\times 20D$, and the boundary conditions (BC) are depicted in Figure 1a. At the inlet, the fluid is at uniform U_∞ free-stream velocity and T_∞ temperature, and outflow BC is employed at the outlet while symmetry BC are applied on top and bottom boundaries. The cylinder of diameter D is assumed to be isothermal ($T=T_\infty$) and impermeable ($u=v=w=0$). In 3D domain, additionally, a depth of πD is considered to incorporate the spanwise effects (Figure 1b). In 3D simulations, periodic boundary conditions are imposed to enclosing spanwise boundaries.

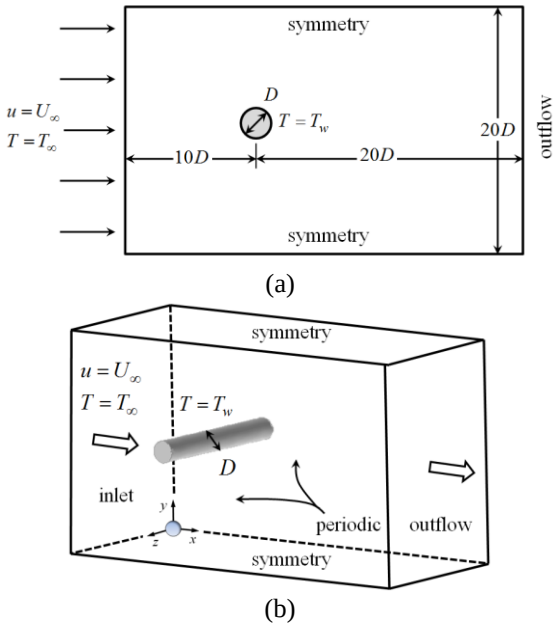

Figure 1. The geometry and the boundary conditions for (a) 2D, (b) 3D numerical models.

The unsteady continuity, momentum, RANS (and LES) and energy equations were solved using FLUENT® 6.3.26. The most common RANS models─SKE, RNGKE, RKE, SKW, SSTKW and RSM─are incorporated into FLUENT® 6.3.26 as a standard feature. The code employs finite volume method (FVM) and provides flexibility in choosing discretization schemes for each equation. The SIMPLE scheme for pressure-velocity coupling was adopted in numerical simulations. "Thermal effects" and "pressure effects" options−which are designed to be used with SKE, RKE, RNGKE and RSM turbulence models in conjunction with EWT model−were activated. These options involve more elaborate models which take into account the thermal and pressure effects within the thermal and hydrodynamic boundary layers of the wake region (Fluent, 2006). For the transient and transport terms the second-order implicit-time-stepping and second-order-upwind scheme were employed, respectively. At the inlet "Turbulent Intensity and Viscosity Ratio" boundary condition is specified. An estimate for the turbulence intensity at the free stream inlet is generally determined experimentally; however, as it will be pointed out later, numerical experimentation was carried out to determine a reasonable inlet conditions. Once a reasonable estimates are introduced, the code computes pertinent boundary values such as k, ε or ω depending on the model used. The discretized equations, along with the initial and boundary conditions, are solved using the segregated (incompressible flow) solver. The convergence criteria imposed to all of the equations was 10^{-5}. The vortex shedding frequency f is obtained from the Fast Fourier Transform of the time-history of the lift coefficient data. The Strouhal number, fD/U_∞, and the cylinder surface-averaged mean drag and rms lift coefficients (C_D, $C_{L,max}$, $C_{L,rms}$), are computed.

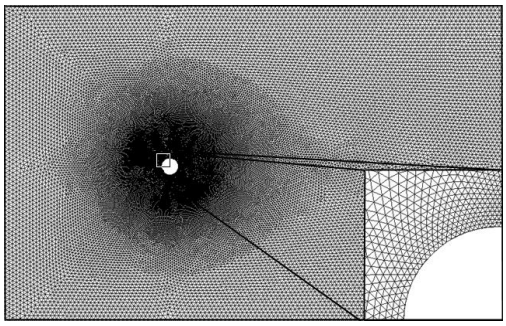

Figure 2. Typical triangular grid for 2D models.

Meshing the domain is the crucial first step to obtain accurate yet meaningful numerical solutions due to resulting steep velocity and temperature gradients within the hydrodynamic and thermal boundary layers. In order to accurately resolve these steep gradients for turbulent flows, a special attention has also been paid to satisfy *y*+ criteria. In the flow, lateral and spanwise directions minimum of 100, 50 and 20 intervals are set. The cylinder wall is meshed between 80 to 200 intervals. In 2D, the domain is meshed with triangular unstructured elements with 1.15 stretching ratio from the cylinder wall towards the exterior boundaries of computational domain (Figure 2). For grid independence study, four grid configurations resulting with 23323, 36080, 91945 and 226485 nodes, were established. A short table depicting grid convergence of the mean heat transfer and flow characteristics with SST and RSM for Re=10000 is presented in Table 1. When considering the computed mean heat and flow characteristics, the grid structure with 91945 was decided to be adequate for the current analysis. For the selected grid configuration, typical cpu-time for 2D simulations ranged between 2 to 3 weeks. In 3D, the same 2D mesh was copied to 20 spanwise intervals which proved to be adequate and consistent with the literature, and volume mesh is performed yielding 1,295,760 cells. The numerical accuracy was further checked by refining and ensuring meshing at the wall was *y*+<1 which in turn especially in 3D computations yielding in some cases up to about 2 million cells.

Table 1. The effect of grid sensitivity study for 2D models (Re=10000, $\Delta\tau$=0.001).

Method	Nodes	C_D	$C_{L,max}$	$C_{L,rms}$	St	Nu
SST	23,323	1.341	1.305	0.902	0.244	67.79
SST	36,080	1.311	1.289	0.885	0.245	67.29
SST	91,945	1.229	1.258	0.843	0.243	66.32
SST	226,485	1.227	1.249	0.837	0.243	66.27
RSM	23,323	1.114	1.110	0.448	0.244	61.73
RSM	36,080	1.141	1.080	0.578	0.241	62.91
RSM	91,945	1.270	0.995	0.689	0.237	64.42
RSM	226,485	1.275	0.984	0.663	0.237	64.27

RESULTS AND DISCUSSIONS

The flow around a cylinder, for Re<50 where frictional forces are dominant, corresponds to slow viscous flow which is symmetric and steady. Laminar asymmetric vortex shedding which is periodic is observed for 50<Re<200 and the flow is unsteady. The vortex formation length shrinks, and the stresses increase in the near wake region. The vortex shedding alters the wake behind the cylinder and affects the flow properties. For 200<Re<300, in the front part of the cylinder, boundary layer is laminar, and it separates over the rear part of the cylinder which breaks up into a turbulent wake. In this range, due to decreasing stresses in the near wake region, a transition from 2D to 3D wake is observed. For Re>1000, the separating shear layers from the cylinder are unstable, and the turbulent transition point moves in upstream direction. Another transition is also observed at the critical Reynolds number ($Re_{cr}=2\times10^5$) where the boundary layer is turbulent before separation and is associated with the drag crisis. The range between 300 to 2×10^5 is known as the subcritical range which is especially of interest to researchers. Thus, the vortex shedding prediction requires turbulence models and its quality strongly depends on the turbulence models used. Nevertheless, relatively few experimental and numerical investigations have been conducted on shear layer transition, mostly because of difficulties in measurement as well as the high demand on computing resources.

Table 2. The effect of turbulence intensity and the viscosity ratio on the heat transfer and flow characteristics (RSM model and $\Delta\tau$=0.005).

Re	I%	β	C_D	$C_{L,rms}$	St	Nu
3900	0.01	0.1	1.052	0.235	0.249	34.15
3900	0.1	0.2	1.065	0.253	0.247	34.42
3900	0.1	5	1.057	0.217	0.247	34.36
3900	0.1	50	1.058	0.217	0.249	34.35
3900	0.5	0.2	1.060	0.236	0.247	34.62
3900	2	0.2	1.194	0.693	0.259	40.63
10000	0.01	0.1	1.086	0.515	0.261	62.65
10000	0.1	0.2	0.921	0.514	0.260	62.62
10000	0.1	5	1.085	0.051	0.267	62.58
10000	0.1	50	1.085	0.506	0.222	62.87
10000	0.5	0.2	1.083	0.514	0.267	64.90
10000	1	0.2	1.092	0.622	0.267	80.26
10000	1	0.3	1.092	0.621	0.260	80.36
10000	2	0.2	1.089	0.617	0.268	80.31

In order to determine the appropriate inlet BC, numerical simulations were performed for a range of turbulence intensity and the viscosity ratio values. For Re=3900 and 10000, a brief summary of the computed mean C_D, $C_{L,rms}$, St number and mean Nu number obtained using 2D RSM models are tabulated in Table 2. FLUENT® recommends the free stream turbulent viscosity ratio ($\beta=\mu_t/\mu$) to be on the order of β<10 for external flows (Fluent, 2006). It is observed that as the turbulence intensity increases, the mean Nusselt number also increases, and the effect of viscosity ratio for fixed

intensity is not significant. The heat transfer and flow characteristics which yielded those of the experimental data closest was determined to be ≈0.1% for the turbulent intensity and ≈0.2 for the viscosity ratio. This set of input values were used in 2D as well as 3D numerical simulations.

Next, to determine the appropriate time step size ($\Delta\tau = U_\infty \Delta t / D$), the simulations were repeated for various time steps. A brief summary of the computed drag, rms lift, St and mean Nu numbers obtained with I=0.1% and β=0.2 conditions are presented for SKW and RSM models in Table 3. It was determined that $\Delta\tau = 0.001$ was sufficient for the unsteady numerical analysis.

Table 3. The effect of time step on the flow and heat transfer characteristics using I=0.1% and β=0.2.

Model	Re	$\Delta\tau$	$C_{D,mean}$	$C_{L,rms}$	St	Nu
SKW	3900	0.010	1.313	0.874	0.232	41.01
SKW	3900	0.005	1.297	0.811	0.231	40.89
SKW	3900	0.001	1.303	0.822	0.229	40.97
RSM	3900	0.010	1.060	0.243	0.245	34.40
RSM	3900	0.005	1.065	0.253	0.247	34,42
RSM	3900	0,001	1.058	0.237	0.243	34.38
RSM	10000	0.010	1.086	0.521	0.261	62.91
RSM	10000	0.005	1.085	0.514	0.260	62.58
RSM	10000	0.001	1.070	0.465	0.257	62.61

Noteworthy Nusselt number correlations, along with the Nu values computed by these correlations are provided for Re=1000, 3900 and 10000 in Table 4. These correlations yield predicted mean and max/min values of 16.22±2.17, 33.85±4.24 and 57.66±4.89 for Re=1000, 3900 and 10000, respectively.

In Table 5, tabulated mean C_D and $C_{L,rms}$ as well as St numbers from experimental, 2D and 3D numerical simulations encountered in the literature are presented for Re=1000. The relevant data are rather rare and do not cover all flow characteristics. Norberg's (2003) data for $C_{L,rms}$ and St number are obtained from correlations derived from a large collection of experimental data. The St numbers from experimental studies, 3D numerical simulations of Patel's (2010) with LES as well as Henderson and Karniadakis's (1995) 3D simulations with spectral element method (SEM) are in agreement at St=0.21. The 2D numerical simulations yield either under or over estimated St numbers. On the other hand, $C_{L,rms}$'s depict a large variation. As the experimental works predict it to be very small (≈0.06), the 2D/3D numerical simulations yield much larger $C_{L,rms}$. Similarly the experimental C_D is determined to be in the order of 1. As 2D simulations with SST and SSTKW models yielded results of the same order magnitute, 2D SEM solution resulted in a very large C_D. In 3D simulations, SST gives a drag coefficient prediction closest to experimental value while simulations with SKE (Patel, 2010), SEM and LES (Patel, 2010) models yield 10-20% higher drag coefficients than that of the experimentally determined value (Franke and Frank, 2002). Relatively few 3D numerical studies yield predictions with mean values of 1.12, 0.2 and 0.21 for C_D, $C_{L,rms}$ and St number, respectively.

Table 4. Nusselt number correlations cited in the literature.

Source	**Correlation**	**Reynolds number**		
		1000	**3900**	**10000**
Fand (1965)	$Nu = (0.35 + 0.34\,Re^{0.5} + 0.15\,Re^{0.58})\,Pr^{0.3}$	17.45	35.85	59.31
Virk (1970)	$Nu = 0.5\,Pe^{0.5}$	18.84	37.21	59.58
Douglas&Churchill (1956)	$Nu = 0.46\,Re^{0.5} + 0.00128\,Re$	15.83	33.72	58.80
Churchill&Bernstein (1977)	$Nu = 0.3 + \frac{0.62\,Re^{1/2}\,Pr^{1/3}}{[1+(0.4/Pr)^{2/3}]^{1/4}}\left[1+\left(\frac{Re}{282000}\right)^{1/2}\right]$	16.02	32.29	53.63
Zhukauskas&Ziugzda (1985)	$Nu = 0.23\,Re^{0.60}$	14.51	32.84	57.77
McAdams (1954)	$Nu = 0.24\,Re^{0.60}$	15.14	34.26	60.29
Reiher (1925)	$Nu = 0.35\,Re^{0.56}$	16.75	35.90	60.82
Hilpert (1933)	$Nu = 0.609\,Re^{0.466}$, $Re < 4000$ $Nu = 0.172\,Re^{0.618}$, $Re > 4000$	15.24	28.73	51.05

In Table 5, tabulated mean C_D and $C_{L,rms}$ as well as St numbers from experimental, 2D and 3D numerical simulations encountered in the literature are presented for Re=1000. The relevant data are rather rare and do not cover all flow characteristics. Norberg's data(2003) for $C_{L,rms}$ and St number are obtained from correlations derived from a large collection of experimental data. The St numbers from experimental studies, 3D numerical simulations of Patel's (2010) with LES as well as Henderson and Karniadakis's (1995) 3D simulations with spectral element method (SEM) are in agreement at St=0.21. The 2D numerical simulations yield either under or over estimated St numbers. On the other hand, $C_{L,rms}$'s depict a large variation. As the experimental works predict it to be very small (≈0.06), the 2D/3D numerical simulations yield much larger $C_{L,rms}$. Similarly the experimental C_D is determined to be in the order of 1. As 2D simulations with SST and

SSTKW models yielded results of the same order magnitute, 2D SEM solution resulted in a very large C_D. In 3D simulations, SST gives a drag coefficient prediction closest to experimental value while simulations with SKE (Patel, 2010), SEM and LES (Patel, 2010) models yield 10-20% higher drag coefficients than that of the experimentally determined value (Franke and Frank, 2002). Relatively few 3D numerical studies yield predictions with mean values of 1.12, 0.2 and 0.21 for C_D, $C_{L,rms}$ and St number, respectively.

Table 5. Literature of flow characteristics for Re=1000.

	Method	C_D	$C_{L,rms}$	St
Experimental				
Franke & Frank (2002)		0.98±0.05		0.210
Rhosko (1961)				0.211
Norberg (2003)			0.058	0.210
2D Studies				
Rahman et al. (2007)	SST	0.995		
Rahman et al. (2007)	SKE			0.151
Rahman et al. (2007)	RKE			0.171
Rahman et al. (2007)]	SSTKW	0.995		0.235
Henderson & Karniadakis (1995)	SEM	1.514	1.049	0.237
3D Studies				
Patel (2010)	SKE	1.117		-
Patel (2010)	SST	0.989		-
Henderson & Karniadakis (1995)	SEM	1.220	0.200	0.210
Patel (2010)	LES*	1.150		0.210

***** Smagorinsky-Lilly+ Dynamic stress

In Table 6, the mean C_D, $C_{L,max}$, $C_{L,rms}$, St and mean Nusselt numbers from our 2D and 3D LES and RANS simulations are tabulated for Re=1000. In 2D, SKE, RKE and RNG models do not produce oscillatory flow characteristics for which the lift coefficients and St number could be determined. However, computed drag coefficients are in the order of that of obtained experimentally (Franke and Frank, 2002). As SKW and SST models yield higher C_D as well as $C_{L,rms}$, the RSM under estimates the mean C_D but yields $C_{L,max}$ and $C_{L,rms}$ compatible with those of the experimental data. The mean Nu numbers computed by all 2D RANS models are within the interval of those predicted by Nusselt number correlations (Table 4). The St numbers computed by SKW, SST and RSM are all 0.228 but slightly over estimated. In 3D simulations, the RNG model also did not produce oscillatory flow characteristic. For this reason, $C_{L,max}$, $C_{L,rms}$ the lift coefficients and St number could not be computed; neverthless, the mean C_D is in agreement with the experimental data (Franke and Frank, 2002)]. The RSM also yielded comparable C_D and $C_{L,rms}$ with those of the experimental data while the St number is over estimated by 20%. On the other hand, the mean C_D predictions of SKW and SST models are 20-30% larger than the experimental prediction (Franke and Frank, 2002) but comparable with those of LES. The SKW, SST and LES models also yield much larger $C_{L,rms}$, but the St numbers are in the order of experimental prediction. The mean Nu numbers of all 3D simulations yielded predictions within the interval of those predicted by Nu number correlations except for RNG which is slightly over estimated.

Table 6. Results of 2D and 3D simulations for Re=1000.

	C_D	$C_{L,max}$	$C_{L,rms}$	St	Nu
2D					
SKE	1.015				17.01
RKE	0.977				16.82
RNG	0.983				17.09
SKW	1.382	1.325	0.954	0.228	17.32
SST	1.381	1.334	0.952	0.228	17.32
RSM	0.873	0.024	0.017	0.228	14.79
3D					
RNG	1.045				18.68
SKW	1.319	1.444	0.680	0.204	17.04
SST	1.308	1.299	0.658	0.200	17.27
RSM	0.941	0.049	0.036	0.243	14.97
LES[1]	1.302	1.169	0.633	0.205	17.11
LES[2]	1.219	0.878	0.457	0.216	17.15

[1] Smagorinsky-Lilly with Dynamic Stress,
[2] Smagorinsky-Lilly

Table 7. Literature of flow characteristics for Re=3900.

	Method	C_D	$C_{L,rms}$	St
Experimental				
Rhosko (1961)				0.215
Norberg (2003)			0.083	0.211
Franke & Frank (2002)		0.98±0.05		0.215±0.050
Parnaudeau et al. (2008)				0.208±0.002
Norgerb (2003)		0.99±0.05		0.215±0.050
Cardell (1993)		0.93±0.005		0.215±0.005
2D Studies				
Rahman et al. (2007)	SST	0.930	0.39	0.228
Rahman et al. (2007)	SKE			0.151
Rahman et al. (2007)	RKE			0.200
Rahman et al. (2007)	SSTKW	0.997		0.250
Young & Ooi (2007)	SKW	1.59	1.17	0.215
Shim et al. (2009)	SST	0.93	0.39	0.228
Beaudan & Moin (1994)	LES	1.74		0.263
3D Studies				
Young & Ooi (2007)	SKW	1.32	0.70	0.223
Shim et al. (2009)	SST	1.27	0.73	0.218
Shim et al. (2009)	SAS-SST	0.99	0.13	0.212
Patel (2010)	SST	0.621		
Patel (2010)	SKE	0.745		
Beaudan & Moin (1994)	LES**	0.96		0.216
Beaudan & Moin (1994)	LES*	1.0		0.203
Patel (2010)	LES*	1.068		0.200
Kravchenko and Moin (2000)	LES	1.04		0.212
Young & Ooi (2007)	LES*	1.03	0.177	0.212
Gopalkrishnan (1993)	VMS-LES	0.99	0.108	0.210
Fröhlich et al. (1998)	LES	1.08		0.216
Franke & Frank (2002)	LES	0.994		0.209
Tremblay et al. (2000)	DNS	1.03		0.220

***** Smagorinsky-Lilly, Dynamic stress

** No model

Experimental, 2D and 3D numerical simulations of the mean C_D and $C_{L,rms}$ as well as St numbers for Re=3900 are summarized in Table 7. Norberg (2003) data listed for $C_{L,rms}$ and St number are computed from the proposed correlations. Experimental studies suggest that C_D ranges in 0.93-0.99 interval while the predicted $C_{L,rms}$ is small and in the order of 0.09. The Strouhal numbers from experimental works fall within 0.215±0.050. The 2D numerical simulations with SSTKW (Rahman et. al., 2007) and SST (Shim et. al., 2009) yield C_D's predicted by experimental works while SKW (Young and Ooi, 2007) and LES (Beaudan & Moin (1994) are over predicted. Although the computed $C_{L,rms}$ values by Rahman et al. (2007) and Shim et al. (2009) are consistent at 0.39, these values are 4.7 times larger than that of the experimental value of 0.083. While SSTKW (Rahman et. al., 2007) and LES (Beaudan and Moin, 1994) over predict, SKE (Rahman et. al., 2007) under predicts the Strouhal number. In 3D numerical simulations, results of Tremblay et al(2000) using DNS yield St number and C_D values which are the most accurate and compatible results with those of the experiments. The SAS-SST (Shim et. al., 2009) as well as all LES models (Young and Ooi, 2007; Fröhlich et. al., 1998; Kravchenkoa and Moin, 2000; Patel, 2010; Beaudan and Moin, 1994; Gopalkrishnan,1993) yielded the drag coefficient and the Strouhal number predictions compatible with those of the experimental data; however, among the researchers that reported $C_{L,rms}$ value, using VMS-LES method by Gopalkrishnan (1993) is the only compatible value with that of the experimental value while SKW (Young and Ooi, 2007) and SST (Shim et. al., 2009) grosly over estimate $C_{L,rms}$.

In Table 8, for Re=3900, C_D, $C_{L,max}$ and $C_{L,rms}$, Strouhal and the mean Nusselt numbers from our 2D and 3D numerical simulations using LES and RANS models are tabulated. The 2D SKE, RKE and RNG models depict similar computational behavior, and they yield C_D's which are consistently under estimated while $C_{L,rms}$ and St number are consistent with those obtained by 3D LES (Smagorinsky-Lilly) simulation. However, the flow characteristics, except for C_L, which are most compatible with 3D simulations in literature (Table 7) are obtained with the RSM model. The SKW and SST models over predict the heat transfer and flow characteristics while other 2D RANS models yield mean Nu number predictions within the interval of those predicted by the Nusselt number correlations. The 3D numerical simulations with the RMS and LES (using Smagorinsky-Lilly with dynamic stress) model produced the most compatible heat transfer and flow

characteristics with respect to the experimental and 3D simulations cited in Table 7. This indicates that the models including complete physical phonemena yield solutions of reasonable accuracy. The mean Nusselt number prediction of Nakamura and Igarashi (2004) for Re=3900 is 35.37; however, the average prediction of three runs with LES (Pasinato, 2008) is 41.27 which over estimates mean Nusselt number by as much as 20% with experimental data. Pasinato (2008) explains this by the ability of the local heat transfer predictions in the separation region which numerical solution and experimental measurements do not match very well.

A relative success in the heat transfer rate predictions using 2D and 3D RANS models, with respect to the the flow characteristics, is due to the fact that the wake region behind the cylinder strongly influences the flow characteristics. Although the local Nusselt number beyond the separations point (in the wake field) also depicts fluctuations due to turbulence effects, both boundary layers befor the seperation points are laminar. Therefore, the time average of these turbulence effects seems to be canceling out the local fluctuation effects for Re≤3900.

Table 8. Results of 2D and 3D simulations for Re=3900.

	C_D	$C_{L,max}$	$C_{L,rms}$	St	Nu
2D					
SKE	0.804	0.220	0.155	0.228	37.62
RKE	0.809	0.245	0.173	0.204	36.95
RNG	0.811	0.254	0.179	0.228	37.95
SKW	1.298	1.162	0.817	0.228	40.91
SST	1.166	0.876	0.610	0.286	41.14
RSM	1.011	0.222	0.156	0.200	33.03
3D					
RNG	0.911	0.371	0.262	0.237	40.42
SKW	1.363	1.450	0.771	0.217	35.81
SST	1.284	1.276	0.603	0.250	35.19
RSM	1.098	0.356	0.248	0.218	33.23
LES[1]	1.291	1.117	0.717	0.210	36.09
LES[2]	1.022	0.667	0.191	0.222	34.17

[1] Smagorinsky-Lilly with Dynamic Stress,
[2] Smagorinsky-Lilly

Table 9. Literature of flow characteristics for Re=10000.

	Method	C_D	$C_{L,rms}$	St
Experimental				
Gopahkrishnan (1993)		1.186	0.384	0.193
Norberg (1994)		1.200	0.4-0.5	0.210
Norberg (2003)			0.411	0.201
2D Studies				
Patel (2010)		1.005		0.176
Bose et al. (2012)		1.670		
3D Studies				
Benim et al. (2008)	SKE	1.260		
Dong et al. (2006)	DNS	1.143	0.448	0.203
Wornom et al. (2011)	VMS-LES*	1.220	0.476	0.200
Benim et al. (2008)	DES	1.120		
Benim et al. (2008)	LES	1.160		
Kim et al. (2015)	LES**	1.133	0.381	0.208
Lu et al. (1997)	LES	1.150	0.460	0.206

* WALE
** k-ε SGS model

For Re=10000, relatively few experimental, 2D/3D numerical simulation predictions of the drag, max and rms lift coefficients and Strouhal numbers encountered in the literature are comparatively presented in Table 9. Experimentally determined C_D values suggests that the drag coefficient be ≈1.2 while the average of the predicted $C_{L,rms}$ and St number would be about 0.415 and 0.204, respectively. Norberg's (2003)experimental data for $C_{L,rms}$ and St are computed from his proposed correlations. The 2D numerical simulations of Patel (2010) and Bose et al. (2012) do not yield reasonable flow characteristics predictions. In the 3D simulations, the computed flow characteristics with LES, DNS and DES are observed to yield results which are compatible with those experimental values. The drag coefficient solution of Benim et al. (2008) (which is the only flow characteristic reported) with SKE and the flow characteristics obtained Wornom et al. (2011) with the VMS-LES method are most compatible with those of the experimental averages.

In Table 10, the C_D, $C_{L,max}$, $C_{L,rms}$, Strouhal and the mean Nusselt numbers from our 2D and 3D numerical simulations using LES and RANS models are tabulated for Re=10000. The 2D numerical simulations with SKE, RKE and RNG models significantly under estimate of the flow characteristics C_D and $C_{L,rms}$ while over estimate C_L and Strouhal number in comparison to experimental/ numerical data presented in Table 9. In fact, from the heat transfer point of view, all RANS models in 2D simulations over predict mean Nusselt numbers (recalling 57.66±4.89) SKW being the worst among the RANS models used. The 3D RANS (except RNG) and LES models yielded consistent drag coefficient and Strouhal number values with respect to the experimental and the 3D numerical results presented in Table 9. Although the C_D, $C_{L,rms}$, St and Nu numbers obtained by SST is compatible with those of LES solutions, $C_{L,rms}$ is over estimated by about 50%. The turbulence models (except for RNG) yielded the mean Nusselt numbers which fall between 52.77 and 62.55 (min and max values predicted from correlations) values.

Table 10. Results of 2D and 3D simulations for Re=10000.

	C_D	$C_{L,max}$	$C_{L,rms}$	St	Nu
2D					
SKE	0.512	0.039	0.026	0.229	65.84
RKE	0.514	0.108	0.077	0.237	65.40
RNG	0.514	0.016	0.012	0.226	67.15
SKW	1.449	0.195	0.132	0.255	87.47
SST	1.229	1.258	0.843	0.243	66.32
RSM	1.270	0.995	0.689	0.237	64.42
3D					
RNG	0.613	0.029	0.090		69.82
SKW	1.259	1.441	0.645	0.201	58.37
SST	1.238	1.110	0.756	0.210	62.17
RSM	1.260	0.723	0.511	0.210	60.21
LES[1]	1.227	1.173	0.471	0.215	62.09
LES[2]	1.223	1.137	0.438	0.214	61.93

[1] Smagorinsky-Lilly with Dynamic Stress,
[2] Smagorinsky-Lilly

The use LES is relatively confined to academic investigations, attempts are being made to employ the method to practical industrial problems. However, the LES and its variants also depict some variations which depend heavily on factors including grid, numerical method employed, BCs and the statistical sampling and convergence criteria. In turbulent flows, specifying BCs accurately is critically important for the success of the simulations. Especially specifying the inlet boundary conditions as real as possible is crucial in many cases because the downstream flow development is largely determined by the inlet behavior. Also when simulating near wall flows accurately, it is essential to resolve the near wall flow structures. In most practical flows, Reynolds number is very large and it would make numerical simulations far too expensive to perform a wall-resolved LES. As far as the computation of the heat transfer rates (mean Nusselt number) are concerned, it was previosly shown that the 2D numerical simulations with RANS models yielded reasonable and comperable mean Nusselt number values for Re≤3900. However, as the Reynolds number is increased, the turbulence effects become significant enough to alter flow field dramatically enough that the 2D RANS models cannot capture. As a result of this inability of 2D RANS models, the computation of the time average mean Nusselt values does not sufficiently reflect the heat transfer rates in which case the use of 3D modeling becomes a requirement.

CONCLUSIONS

Unsteady turbulent flow and heat transfer from a single isothermal cylinder placed in crossflow of air are comparatively investigated for Re=1000, 3900 and 10000 by 2D- and 3D-RANS and LES turbulence models avaiable in FLUENT® 6.3.26. The 2D-simulations are carried out for SKE, RNG, RKE, SKW, SST and RSM turbulence RANS models, and for 3D-simulations the RNG, SKW, SST and RSM models and two LES (Smagorinsky-Lilly with/without dynamic stress) models were used. The influence of the turbulence models on the mean flow characteristics (St, C_D, $C_{L,rms}$) and heat transfer via the mean Nusselt number is assessed with respect to the published experimental and numerical data. The study concludes the following:

(i) The 2D RANS models are not consistent in predicting all of the flow characteristics which is attributed to the three-dimensionality nature of the flow. The RNG, RKE and SKE models in 2D simulations yield almost identical results. The overall performance of the RSM model is slightly better than other RANS models since the model is physically more complete by the inclusion of additional equations for the Reynolds stresses. The 2D-RSM could be considered an alternative for 3D computations, but the compuational cost is yet reasonably higher than the other RANS models. Nevertheless, despite 3D wakes occuring in the Reynolds number range studied here, the 2D RANS simulations would still provide invaluable preliminary information before attempting expensive 3D simulations.

(ii) LES models yield the most reasonable flow characteristics and heat transfer rates in the flow conditions ($10^3 \leq Re \leq 10^4$) considered; however, the performance of LES is also influenced by a number of factors one of which is the accurate description of the turbulence fluctuations at the inlet. In this study, the Smagorinsky-Lilly model yielded flow and heat transfer characteristics slightly better for all Reynolds numbers used in the study.

(iii) Simulations for Re=1000 and Re=3900, using 2D-RANS models, resulted in the mean Nuselt number predictions accurate within the cited experimental and numerical predictions in the literature. When the mean heat transfer rate is the primary computational concern, the 2D RANS models yield numerical analysis with sufficient accuracy. However, for Re=10000, the SKE, RKE, RNG and RSM models yields the mean Nusselt values within the Nusselt number range predicted by the presented correlations. In 3D models, the RNG model consistently over estimated mean Nusselt numbers while the other models also resulted in mean Nu values within the Nu number range predicted by the correlations.

REFERENCES

Achenbach E., 1968, Distribution of local pressure and skin friction around a circular cylinder in cross-flow up to Re=5×106, *Journal of Fluid Mechanics*, 34, 625-639.

Ahmed G. R. and Yonanovich M. M., 1997, Experimental Study of Forced Convection From Isothermal Circular and Square Cylinders and Toroid, *Journal of Heat Transfer*, 119, 70-79.

Beaudan P. and Moin P., 1994, Numerical experiments on the flow past a circular cylinder at sub–critical Reynolds number, *Technical Report TF-62*, Stanford University.

Benim A. C., Pasqualotto E. and Suh S. G., 2008, Modelling turbulent flow past a circular cylinder by RANS, URANS, LES and DES, *Progress in Computational Fluid Dynamics*, 8, 299-307.

Breuer M., 1998, Large Eddy Simulations of the subcritical flow past a circular cylinder: numerical and modeling aspects, *International Journal of Numerical Methods in Fluids*, 28, 1281-1302.

Bose S. T., Wang B. C. and Saeedi M. D., 2012, Prediction of unsteady heat transfer from a cylinder in crossflow, *Center for Turbulent Research Proceedings, Summer Prog*, 107-116.

Boulos M. I. and Pei D. C., 1973, Heat and mass transfer from cylinders to a turbulent fluid stream—a critical review, *Canadian Journal of Chemical Engineering*, 51, 673-679.

Cardell G. S., 1993, *Flow past a circular cylinder with a permeable splitter plate*, PhD Thesis, Graduate Aeronautical Lab., California Inst. of Tech, USA.

Celik I. and Shaffer F. D., 1995, Long time averaged solutions of turbulent flow past a circular cylinder, *Journal of Wind Engineering and Industrial Aerodynamics*, 56, 185-212.

Churchill S. W. and Bernstein N. M., 1977, A Correlating Equation for Forced Convection From Gases and Liquids to a Circular Cylinder in Crossflow, *Journal of Heat Transfer*, 99, 300-306.

Dong S., Karniadakis G. E., Ekmekci A. and Rockwell D., 2006, A combined direct numerical simulation–particle image velocimetry study of the turbulent near wake, *Journal of Fluid Mechanics*, 569, 185-207.

Douglas W. J. M. and Churchill S. W., 1956, Recorrelation of Data for Convective Heat Transfer Between Gases and Single Cylinders With Large Temperature Differences, *Chemical Engineering Progress Symposium Series*, 52, 23-28.

Fand R. M., 1965, Heat transfer by forced convection from a cylinder to water in crossflow, *International Journal of Heat Mass Transfer*, 8, 995-1010.

Fluent Inc., 2006, *Fluent 6.3 User's Guide*, Lebanon, USA.

Franke J. and Frank W., 2002, Large eddy simulation of the flow past a circular cylinder at Re_D=3900, *Journal of Wind Engineering and Industrial Aerodynamics*, 90, 1191-1206.

Fröhlich J., Rodi W., Kessler Ph., Parpais S., Bertoglio J. P. and Laurence, D, 1998, Large Eddy Simulation of Flow around Circular Cylinders on Structured and Unstructured Grids Numerical Flow Simulation I, *Notes on Numerical Fluid Mechanics*, 66, 319-338.

Gerrard J. H., 1961, An experimental investigation of the oscillating lift and drag of a circular cylinder shedding turbulent vortices, *Journal of Fluid Mechanics*, 11, 244-256.

Gopalkrishnan R., 1993, Vortex-induced Forces on Oscillating Bluff Cylinders, PhD Thesis, MIT, USA.

Henderson R. D. and Karniadakis G. E., 1995, Unstructured spectral element methods for simulation of turbulent flows, *Journal of Computational Physics*, 122, 191-217.

Hilpert R., 1933, Heat Transfer from Cylinders, *Forsch. Geb. Ingenieurwes*, 4, 215-220.

Kacker S. C., Pennington B. and Hill R. S., 1974, Fluctuating Lift Coefficient for a Circular Cylinder in Cross Flows, *Journal of Mechanical Engineering Science*, 16, 215-224.

Kalro V. and Tezduyar T., 1997, Parallel 3D computation of unsteady flows around circular cylinders, *Parallel Computing*, 23, 1235-1248.

Kim S., Wilson P. A. and Chen Z., 2012, Effect of spanwise discretisation on turbulent flow past a circular

cylinder, *International Journal of Maritime Engineering*, 158, 69-76.

Kim S., Wilson P. A. and Chen Z., 2015, Large-eddy simulation of the turbulent near wake behind a circular cylinder: Reynolds number effect, *Applied Ocean Research*, 49, 1-8.

Kravchenkoa A. G. and Moin P, 2000, Numerical studies of flow over a circular cylinder at Re_D=3900, *Physics of Fluids*, 12, 403-417.

Launder B. E. and Spalding D. B, 1972, *Lectures in Mathematical Models of Turbulence*, London, England.

Lu X., Dalton C. and Zhang J., 1997, Application of large eddy simulation to an oscillating flow past a circular cylinder, *Journal of Fluids Engineering*, 119, 519-525.

Lysenko D. A., Ertesvag I. S. and Rian K. E., 2012, Large-Eddy Simulation of the Flow Over a Circular Cylinder at Reynolds Number 3900 Using the OpenFOAM Toolbox, *Flow Turbulence and Combustion*, 89, 491-518.

McAdams W. H., 1954, *Heat Transmission*, McGraw-Hill, New York, USA.

Menter F. R., 1994, Two-Equation Eddy-Viscosity Turbulence Models for Engineering Applications, *American Institute Aeronatics and Austronatics Journal*, 32, 1598-1605.

Morgan V. T., 1975, The Overall Convective Heat Transfer from Smooth Circular Cylinders, In: Thomas F. Irvine and James P. Hartnett, Editor(s), *Advances in Heat Transfer*, 11, 199-264.

Mustto A. A. and Bodstein G. C. R., 2011, Subgrid-Scale Modeling of Turbulent Flow Around Circular Cylinder by Mesh-Free Vortex Method, *Engineering Applied Computational Fluid Mechanics*, 5, 259-275.

Nakamura H. and Igarashi T., 2004, Unsteady heat transfer from a circular cylinder for Reynolds numbers from 3000 to 15,000, *Internationa Journal of Heat and Fluid Flow*, 25, 741-748.

Niemann H. J. and Hölscher N., 1990, A review of recent experiments on the flow of past circular cylinders, *Journal of Wind Engineering and Industrial Aerodynamics*, 33, 197-209.

Norberg C. and Sunden B., 1987, Turbulence and Reynolds number effects on the flow and fluid forces on a single cylinder in cross flow, *Journal of Fluids and Structures*, 1, 337-357.

Norberg C, 1994, An experimental investigation of the flow around a circular cylinder: influence of aspect ratio, *Journal of Fluid Mechanics*, 258, 287-316.

Norberg C., 2003, Fluctuating lift on a circular cylinder: review and new measurements, *Journal of Fluids and Structures*, 17, 57-96.

Ong M. C., Utnes T., Holmedal L. E., Myrhaug D. and Pettersen B., 2009, Numerical simulation of flow around a smooth circular cylinder at very high Reynolds numbers, *Marine Structures*, 22, 142-153.

Ouvrard H., Koobus B., Dervieux A. and Salvetti M. V., 2010, Classical and variational multiscale LES of the flow around a circular cylinder on unstructured grids, *Computers and Fluids*, 39, 1083-1094.

Parnaudeau P., Carlier J., Heitz D. and Lamballais E., 2008, Experimental and numerical studies of the flow over a circular cylinder at Reynolds number 3900, *Physics of Fluids*, 20, 085101.

Pasinato H. D., 2008, Large-Eddy Simulation of the Flow and Thermal Fields Past a Circular Cylinder, *Mecánica, Comput XXVII, Numerical Simulation of Turbulent Flows*, 249-264.

Patel Y., 2010, *Numerical Investigation of Flow Past a Circular Cylinder and in a Staggered Tube Bundle Using Various Turbulence Models*, MS Thesis, Lappeenranta University of Technology.

Rahman M., Karim M. and Alim A., 2007, Numerical investigation of unsteady flow past a circular cylinder using 2-D finite volume method, *Journal of Naval Architecture and Marine Engineering*, 4, 27-42.

Reiher H., 1925, Der warmeubergang von stromender luft an rohrbundel in kreuzstrom, *VDI Forschungsheft*, 269 (1925) 47-51.

Roshko A., 1961, Experiments on the flow past a circular cylinder at very high Reynolds number, *Journal of Fluid Mechanics*, 10, 345-356.

Saghafian M., Stansby P. K., Saidi M. S. and Apsley D. D., 2003, Simulation of turbulent flows around a circular cylinder using nonlinear eddy-viscosity modelling: steady and oscillatory ambient flows, *Journal of Fluids and Structures*, 17, 1213-1236.

Scholten J. W. and Murray D. B., 1998, Unsteady heat transfer and velocity of a cylinder in cross flow—I. Low freestream turbulence, *International Journal of Heat Mass Transfer*, 41, 1139-1148.

Scholten J. W. and Murray D. B., 1998, Unsteady heat transfer and velocity of a cylinder in cross flow—II. High freestream turbulence, *International Journal of Heat Mass Transfer*, 41, 1149-1156.

Selvam R. P., 1997, Finite element modeling of flow around a circular cylinder using LES, *Journal of Wind Engineering and Industrial Aerodynamics*, 67, 129-139.

Shih T. H., Liou W. W., Shabbir A., Yang Z. and Zhu, J., 1995, A New k-ε Eddy-Viscosity Model for High Reynolds Number Turbulent Flows, *Compututers and Fluids*, 24, 227-238.

Shim Y. M., Sharma R. N. and Richards P. J., 2009, Numerical study of the flow over a circular cylinder in the near wake at Reynolds number 3900, *39th AIAA Fluid Dynamics Conference 22 - 25 June 2009*, AIAA 2009-4160, San Antonio, Texas, TX, 1-13.

Sidebottom W., Ooi A. and Jones D., 2015, A Parametric Study of Turbulent Flow Past a Circular Cylinder Using Large Eddy Simulation, *Journal of Fluids Engineering*, 137, 091202.

Tremblay F., Manhart M. and Friedrich R., 2000, DNS of flow around a circular cylinder at a subcritical Reynolds number with cartesian grids. *In: Proceedings of the 8th European Turbulence Conference, Barcelona, Spain, EUROMECH, CIMNE, 27–30 June*, 659–662.

Ünal U. O., Atlar M. and Gören Ö., 2010, Effect of turbulence modelling on the computation of the near-wake flow of a circular cylinder, *Ocean Engineering*, 37, 387-399.

Virk P. S., 1970, Heat Transfer From the Rear of a Cylinder in Transverse Flow, *Journal of Heat Transfer*, 92, 206-207.

Wilcox D. C., 1998, Turbulence Modeling for CFD, *DCW Industries Inc.*, La Canada, California, 73-163.

Williamson C. H. K. and Govardhan R., 2004, Vortex-induced vibrations, *Annual Review of Fluid Mechanics*, 36, 413-455.

Wornom S., Ouvrard H., Salvetti M. V., Koobus B. and Dervieux A., 2011, Variational multiscale large-eddy simulations of the flow past a circular cylinder: Reynolds number effects, *Computers and Fluids*, 47, 44-50.

Yakhot V. and Orszag, S. A., 1986, Renormalization Group Analysis of Turbulence: I. Basic Theory, *Journal of Scientific Computing*, 1, 3-51.

Young M. E. and Ooi A., 2007, Comparative assessment of LES and URANS for flow over a cylinder at a Reynolds number of 3900, *15th Australasian Fluid Mechanics. Conf. The University of Sydney*, 2-7 December, Sydney, Australia.

Zhukauskas A. and Ziugzda J., 1985, Heat Transfer of a Cylinder in Crossflow, *Hemisphere Publishing Corporation*, New York, USA.